Griffiths, D. V. & Fenton, G. A. (2001). *Géotechnique* **51**, No. 4, 351–359

Bearing capacity of spatially random soil: the undrained clay Prandtl problem revisited

D. V. GRIFFITHS* and G. A. FENTON†

By merging elasto-plastic finite element analysis with random field theory, an investigation has been performed into the bearing capacity of undrained clays with spatially varying shear strength. The object of the investigation is to determine the extent to which variance and spatial correlation of the soil's undrained shear strength impact on the statistics of the bearing capacity. Throughout this study, bearing capacity results are expressed in terms of the bearing capacity factor, N_c, in relation to the mean undrained strength. For low coefficients of variation of shear strength, the expected value of the bearing capacity factor tends to the Prandtl solution of $N_c = 5{\cdot}14$. For higher values of the coefficient of variation, however, the expected value of the bearing capacity factor falls quite steeply. The spatial correlation length is also shown to be an important parameter that cannot be ignored. The results of Monte Carlo simulations on this non-linear problem are presented in the form of histograms, which enable the interpretation to be expressed in a probabilistic context. Results obtained in this study help to explain the well-known requirement that bearing capacity calculations require relatively high factors of safety compared with other branches of geotechnical design.

KEYWORDS: bearing capacity; limit state design/analysis; numerical modelling; plasticity; shear strength; statistical analysis

En associant une analyse d'éléments finis élasto-plastiques et une théorie du champ aléatoire, nous avons enquêté sur la capacité porteuse des argiles non drainées ayant une résistance au cisaillement variant dans l'espace. Cette investigation a pour but de déterminer les effets sur les statistiques de capacité porteuse de la variance et de la corrélation spatiale de la résistance au cisaillement non drainé du sol. Tout au long de cette étude, nous exprimons les valeurs de capacité porteuse en termes de facteur de capacité porteuse, N_c, par rapport au moyen de résistance non drainée. Pour les coefficients bas de variation de résistance au cisaillement, la valeur attendue du facteur de capacité porteuse tend à la solution de Prandtl de $N_c = 5{\cdot}14$. Cependant, pour des valeurs plus élevées du coefficient de variation, la valeur attendue du facteur de capacité porteuse baisse de manière assez marquée. Nous montrons également que la longueur de la corrélation spatiale est un paramètre important qui ne peut être négligé. Nous présentons les résultats des simulations de Monte-Carlo sur ce problème non linéaire sous forme d'histogrammes, ce qui permet d'exprimer l'interprétation dans un contexte probabiliste. Les résultats obtenus dans cette étude aident à expliquer une nécessité bien connue : les calculs de capacité porteuse demandent des facteurs de sécurité relativement élevés par rapport aux autres branches de conception géophysique.

INTRODUCTION

The paper presents results obtained using a program developed by the authors that merges non-linear elasto-plastic finite element analysis (e.g. Smith & Griffiths, 1998) with random field theory (e.g. Vanmarcke, 1984; Fenton, 1990). The program computes the bearing capacity of a smooth rigid strip footing (plane strain) at the surface of an undrained clay soil with a shear strength $c_u(\phi_u = 0)$ defined by a spatially varying random field.

Rather than deal with the actual bearing capacity, this study focuses on the dimensionless bearing capacity factor N_c, defined as

$$N_c = \frac{q_f}{c_u} \tag{1}$$

where q_f is the bearing capacity and c_u is the undrained shear strength of the soil beneath the footing. For a homogeneous soil with a constant undrained shear strength, N_c is given by the Prandtl solution, and equals $2 + \pi$ or 5·14.

In this study, the variability of the undrained shear strength is assumed to be characterised by a log-normal distribution with three parameters as shown in Table 1.

An explanation and justification for the use of the log-normal distribution is given in the next section. While the mean and standard deviation are familiar concepts to most engineers, and can conveniently be expressed in terms of the dimensionless coefficient of variation defined as

Table 1. Shear strength properties

		Units
Mean	μ_{c_u}	kN/m^2
Standard Deviation	σ_{c_u}	kN/m^2
Spatial Correlation Length	$\theta_{\ln c_u}$	m

$$\mathrm{COV}_{c_u} = \frac{\sigma_{c_u}}{\mu_{c_u}} \tag{2}$$

the spatial correlation length is perhaps less well known. This parameter, which has units of length, describes the distance over which the spatially random values will tend to be correlated in the underlying Gaussian field. Thus a large value of $\theta_{\ln c_u}$ will imply a smoothly varying field, while a small value will imply a ragged field. Since the actual undrained shear field is assumed to be log-normally distributed, taking its logarithm yields an 'underlying' normally distributed (or Gaussian) field. The spatial correlation length is measured with respect to this underlying field: that is, with respect to $\ln c_u$. In particular, the spatial correlation length can be estimated from a set of shear strength data taken over some spatial region simply by performing the statistical analyses on the log-data. In practice, however, $\theta_{\ln c_u}$ is not much different in magnitude from the correlation length in real space, and, for most purposes, θ_{c_u} and $\theta_{\ln c_u}$ are interchangeable give their inherent uncertainty in the first place. In this paper a dimensionless spatial correlation length measure Θ_{c_u} is used, where

$$\Theta_{c_u} = \frac{\theta_{\ln c_u}}{B} \tag{3}$$

and B is the width of the strip footing.

In the parametric studies that follow, the mean strength (μ_{c_u})

Manuscript received 13 April 2000; revised manuscript accepted 2 January 2001.
Discussion on this paper closes 1 November 2001, for further details see p. ibc.

* Colorado School of Mines, USA.
† Dalhousie University, Canada.

has been held constant at 100 kN/m^2, while the standard deviation (σ_{c_u}) and spatial correlation length (Θ_{c_u}) are varied systematically.

It has been suggested (e.g. Lee *et al.*, 1983; Kulhawy *et al.*, 1991; Duncan, 2000) that typical COV_{c_u} values for the undrained shear strength lie in the range 0·1–0·5; however, the spatial correlation length is less well documented, especially in the horizontal direction, and may well exhibit anisotropy. While the analysis tools used in this study are capable of modelling an anistropic spatial correlation field, all the results presented in this paper assume that Θ_{c_u} is isotropic.

For each set of assumed statistical properties given by COV_{c_u} and Θ_{c_u}, Monte Carlo simulations have been performed involving n_{sim} repetitions or 'realisations' of the shear strength random field and the subsequent finite-element analysis of bearing capacity. This means that each realisation, while having the same underlying statistics, leads to a quite different spatial pattern of shear strength values beneath the footing. Each realisation therefore leads to a different value of the bearing capacity and, after normalisation by the mean undrained shear strength, a different value of the bearing capacity factor,

$$N_{c_i} = \frac{q_{f_i}}{\mu_{c_u}} \qquad i = 1, 2, \ldots, n_{\mathrm{sim}} \tag{4}$$

In this study $n_{\mathrm{sim}} = 1000$, and once the bearing capacity factors from all the realisations have been accumulated, they in turn can be subjected to statistical analysis. Estimated (sample) mean bearing capacities will have a standard error (± one standard deviation) equal to the sample standard deviation times $1/\sqrt{n_{\mathrm{sim}}} = 1/\sqrt{1000} = 0{\cdot}032$, or about 3% of the sample standard deviation. Similarly, the estimated variance will have a standard error equal to the sample variance times $\sqrt{(2/(n_{\mathrm{sim}} - 1))} = \sqrt{(2/99)} = 0{\cdot}045$, or about 4% of the sample variance. This means that estimated quantities will generally be within about 5% of the true quantities, statistically speaking.

Of particular interest in the present study is the probability that the actual bearing capacity factor, N_c, as defined in equation (4), will be less than the Prandtl value of 5·14 that would be obtained assuming a homogeneous soil with undrained shear strength everywhere equal to the mean value μ_{c_u}.

REVIEW OF THE LOG-NORMAL DISTRIBUTION

A log-normal distribution for the undrained shear strength, c_u, has been adopted in this study, meaning that $\ln c_u$ is normally distributed. If the mean and standard deviation of the undrained shear strength are μ_{c_u} and σ_{c_u} respectively, then the standard deviation and mean of the underlying normal distribution of $\ln c_u$ are given by

$$\sigma_{\ln c_u} = \sqrt{\left\{\ln\left[1 + \left(\frac{\sigma_{c_u}}{\mu_{c_u}}\right)^2\right]\right\}} \tag{5}$$

$$\mu_{\ln c_u} = \ln \mu_{c_u} - \tfrac{1}{2}\sigma^2_{\ln c_u} \tag{6}$$

and the probability density function of the lognormal distribution is given by

$$f(c_u) = \frac{1}{c_u \sigma_{\ln c_u}\sqrt{2\pi}} \exp\left[-\tfrac{1}{2}\left(\frac{\ln c_u - \mu_{\ln c_u}}{\sigma_{\ln c_u}}\right)^2\right] \tag{7}$$

In terms of the properties of the underlying normal distribution, the properties of the log-normal distribution can therefore be summarised as follows:

$$\mu_{c_u} = \exp\left(\mu_{\ln c_u} + \tfrac{1}{2}\sigma^2_{\ln c_u}\right) \tag{8}$$

$$\sigma_{c_u} = \mu_{c_u}\sqrt{[\exp(\sigma^2_{\ln c_u}) - 1]} \tag{9}$$

$$\text{Median} = \exp(\mu_{\ln c_u}) \tag{10}$$

$$\text{Mode} = \exp(\mu_{\ln c_u} - \sigma^2_{\ln c_u}) \tag{11}$$

Use of the log-normal distribution, as opposed to the more familiar normal distribution, or even some other more complex distribution, is based on the following arguments: First, there is a lack of exhaustive field data that would be necessary to conclusively support one kind of distribution over another. However, there is some evidence from the field to support the log-normal distribution for some soil properties (e.g. Hoeksema & Kitanidis, 1985; Sudicky, 1986). Use of the log-normal distribution is also based on the simplicity and familiarity of it two-parameters description. Second, and perhaps more importantly from a physical standpoint, the log-normal distribution is strictly non-negative, unlike the normal distribution, and so there is no possibility of generating properties with meaningless negative values, particularly in the extremes of the distribution (which may be important from a reliabilty standpoint). It might also be noted that a log-normal distribution looks quite similar to a normal distribution for low values of the COV.

Lee *et al.* (1983) comment that the 'normal or log-normal distributions are adequate for the large majority of geotechnical data'; however, Harr (1987) finds the unbounded nature of the upper end of the log-normal distribution objectionable. The potential for the log-normal distribution to generate very high property values (albeit with a low probability) is not considered a serious flaw, especially in a study involving the shear strength of heterogeneous soil that is spatially distributed (what is the shear strength of a point that happens to fall inside a boulder of granite?). It is certainly possible that a soil deposit will contain occasional inclusions of very strongly cemented material.

A typical log-normal distribution based on equation (7) with mean $\mu_{c_u} = 100$ kN/m^2 and standard deviation $\sigma_{c_u} = 50$ kN/m^2 ($\mathrm{COV}_{c_u} = 0{\cdot}5$) is shown in Fig. 1. From equations (5) and (6) it is easily shown that the underlying 'normal' statistics are given by $\sigma_{\ln c_u} = 0{\cdot}472$ and $\mu_{\ln c_u} = 4{\cdot}494$. Highlighted also on the figure are the median and mode of the distribution, which can be shown from equations (10) and (11) to equal, respectively, 89·4 kN/m^2 and 71·6 kN/m^2. The skewed nature of the log-normal distribution always results in the mode, median and mean being in the sequence indicated. In a log-normal distribution the median is always smaller than the mean, and this will have implications for the probabilistic interpretation of the bearing capacity results described later in the paper.

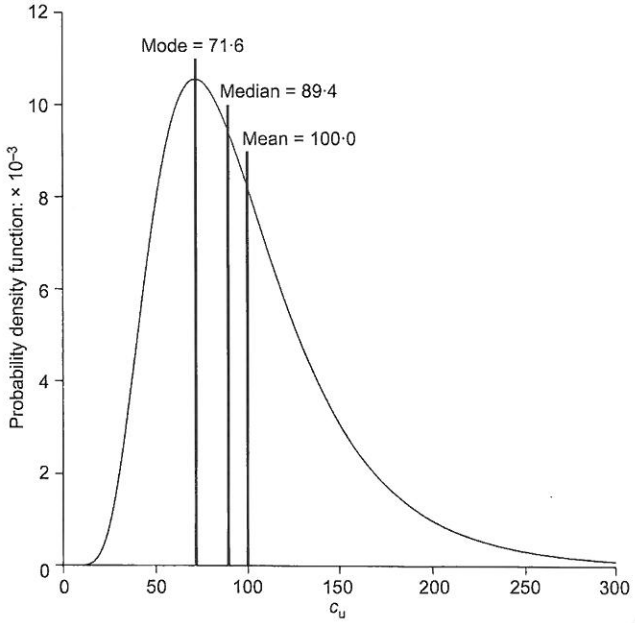

Fig. 1. Typical log-normal distribution of undrained shear strength with a mean of 100 and standard deviation of 50 ($\mathrm{COV}_{c_u} = 0{\cdot}5$). All units are in kN/m^2

BRIEF DESCRIPTION OF THE FE METHOD USED

The bearing capacity analyses use an elastic-perfectly plastic stress–strain law with a Tresca failure criterion. Plastic stress redistribution is accomplished using a viscoplastic algorithm. The program uses 8-node quadrilateral elements and reduced Gaussian integration in both the stiffness and stress redistribution parts of the algorithm. The theoretical basis of the method is described more fully in Chapter 6 of the text by Smith & Griffiths (1998).

The finite element model incorporates three parameters: Young's modulus (E), Poisson's ration (ν), and the undrained shear strength (c_u). The methodology allows for random distributions of all three parameters; however, in the present study E and ν are held constant while c_u is randomised.

A mesh is shown in Fig. 2 consisting of 1000 elements, with 50 columns and 20 rows. Each element is square, and the strip footing has a width of 10 elements.

At the ith realisation of the Monte Carlo process, the footing is incrementally displaced vertically (δ_v) into the soil, and the sum of the nodal reactions (Q_i) is back-figured from the converged stress state. When the sum of the nodal reactions levels out to within a quite strict tolerance, 'failure' is said to have occurred, and the sum of the nodal reactions divided by the footing area is the 'bearing capacity' ($q_{f_i} = Q_{f_i}/B$) of that particular realisation.

A BRIEF DESCRIPTION OF THE RANDOM FIELD MODEL

The undrained shear strength is obtained through the transformation

$$c_{u_i} = \exp(\mu_{\ln c_u} + \sigma_{\ln c_u} g_i) \tag{12}$$

in which c_{u_i} is the undrained shear strength assigned to the ith element, g_i is the local average of a standard Gaussian random field, g, over the domain of the ith element, and $\mu_{\ln c_u}$ and $\sigma_{\ln c_u}$ are the mean and standard deviation of the logarithm of c_u (obtained from the 'point' mean and standard deviation μ_{c_u} and σ_{c_u} after local averaging).

The LAS technique (Fenton, 1990; Fenton & Vanmarcke, 1990) generates realisations of the local averages, g_i, that are derived from the random field g having zero mean, unit variance, and a spatial correlation length $\theta_{\ln c_u}$. As the spatial correlation length tends to infinity, g_i becomes equal to g_j for all elements i and j: that is, the field of shear strengths tends to become uniform for each realisation. At the other extreme, as the spatial correlation length tends to zero, g_i and g_j become independent for all $i \neq j$: the soil's undrained shear strength changes rapidly from point to point. In the present study, a Markovian spatial correlation function was used, of the form

$$\rho(|\tau|) = \exp\left(-\frac{2}{\theta_{\ln c_u}}|\tau|\right) \tag{13}$$

where ρ is the correlation coefficient between the logarithm of the undrained strength values at any two points separated by a distance τ in a random field with spatial correlation length $\theta_{\ln c_u}$.

In the two-dimensional analysis presented in this paper, the spatial correlation lengths in the vertical and horizontal directions are taken to be equal (isotropic) for simplicity. Fenton (1999) examined CPT data in relation to random field modeling; however, the actual spatial correlation structure of soil deposits is not usually well known, especially in the horizontal direction (e.g. Asaoka & Grivas, 1982; de Marsily, 1985; DeGroot & Baecher, 1993). In this paper therefore, a parametric approach has been employed to study the influence of $\theta_{\ln c_u}$.

The plane strain model used herein implies that the out-of-plane spatial correlation length is infinite: thus soil properties are constant in this direction. This is clearly a deficiency. However, previous studies by the authors (Griffiths & Fenton, 1997) involving seepage through two- and three-dimensional random fields have indicated that the difference may not be very great. The role of the third dimension is an area of ongoing research by the authors.

A local averaging process has been included in the formulation to take full account of the level of mesh discretisation, and the size of the finite elements onto which the random field is to be mapped. Local averaging preserves the mean, but reduces the standard deviation of the underlying normal field to a 'target' value. The amount by which the standard deviation is reduced depends on the size of the elements and the nature of the spatial correlation function governing the field. More specifically, there is a function called the 'variance function', which can be derived from the correlation function, and which governs the rate at which the standard deviation drops as the averaging domain grows larger. The interested reader is referred to Vanmarcke (1984) for a detailed description of this formulation.

Although the mean of the underlying Gaussian field is

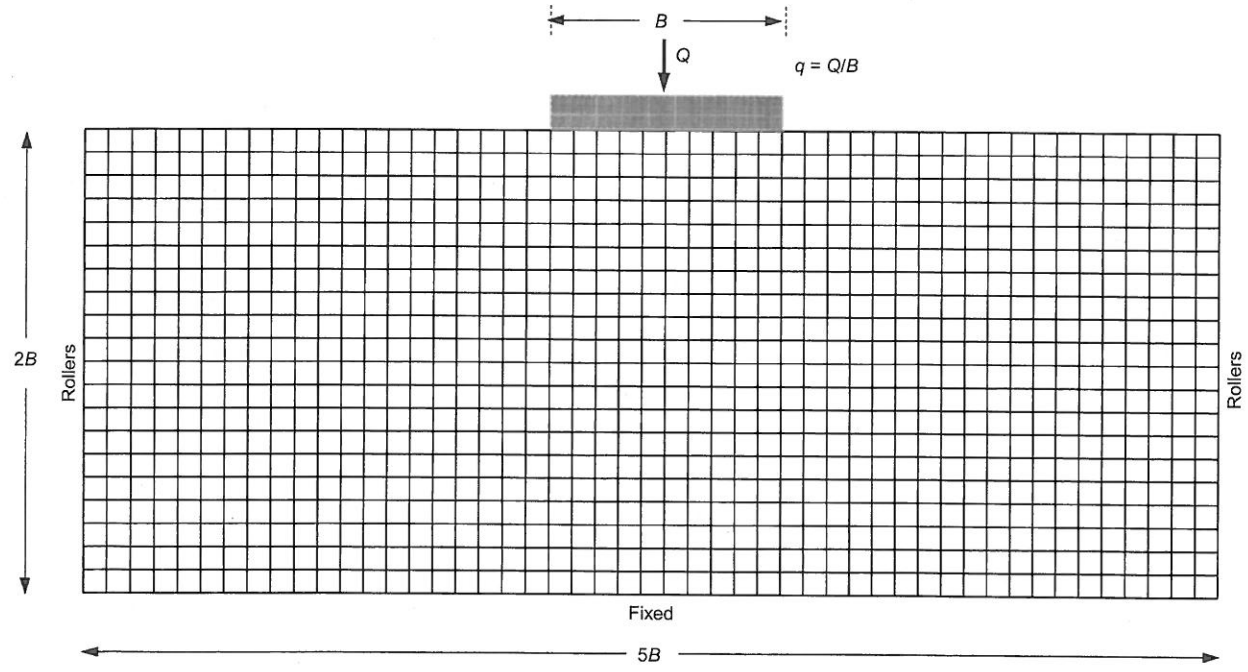

Fig. 2. Mesh used in probabilistic bearing capacity analyses

unaltered by local averaging, equations (8) and (9) indicate that since both the mean and standard deviation of the log-normal field are functions of $\sigma_{\ln c_u}$ they will both be reduced by the local averaging process. Thus the coarser the mesh, the greater the reduction in the 'target' statistics from their nominal 'point' values. This local averaging approach is fully implemented in this study, and removes any 'mesh effects' that might otherwise be present. It might also be noted that this approach is quite consistent with the philosophy of the finite element method, in which finer meshes resolve the finer variations in the stress and material property fields.

PARAMETRIC STUDIES

Analyses were performed using the mesh of Fig. 2 with the input parameters in the following ranges:

$$0{\cdot}125 \leqslant \Theta_{c_u} < \infty \qquad (14)$$

$$0{\cdot}125 \leqslant \mathrm{COV}_{c_u} \leqslant 4$$

To indicate the nature of the different solutions obtained at each realisation of the Monte Carlo process, load/deformation results for ten typical realisations of the footing analysis are shown in Fig. 3 for the case when $\Theta_{c_u} = 1$ and $\mathrm{COV}_{c_u} = 1$. The average stress, q, under the footing has been non-dimensionalised by dividing it by the mean undrained shear strength, μ_{c_u}. The reader should bear in mind the Prandtl solution of 5·14 when viewing this figure. It is clear that a majority of the curves flatten out at bearing capacity values below the Prandtl solution. This trend will be confirmed in all the results shown in this paper.

Figure 4 shows a typical deformed mesh at failure with a superimposed greyscale corresponding to $\Theta_{c_u} = 1$, in which lighter regions indicated stronger soil and darker regions indicated weaker soil. In this case the dark zones and the light zones are roughly the width of the footing itself, and it appears that the weak (dark) region near the ground surface to the right of the footing has triggered a quite non-symmetric failure mechanism. The shape of the non-symmetric mechanism is emphasised further by the plot of displacement vectors for the same realisation, shown in Fig. 5.

For each combination of Θ_{c_u} and COV_{c_u}, $n_{\mathrm{sim}} = 1000$ realisations of the Monte Carlo process were performed, and the estimated mean (m_{N_c}) and standard deviation (s_{N_c}) of the resulting 1000 bearing capacity factors from equation (4) were computed.

Figure 6(a) shows how the estimated mean bearing capacity factor, m_{N_c}, varies with Θ_{c_u} and COV_{c_u}. The plot confirms that,

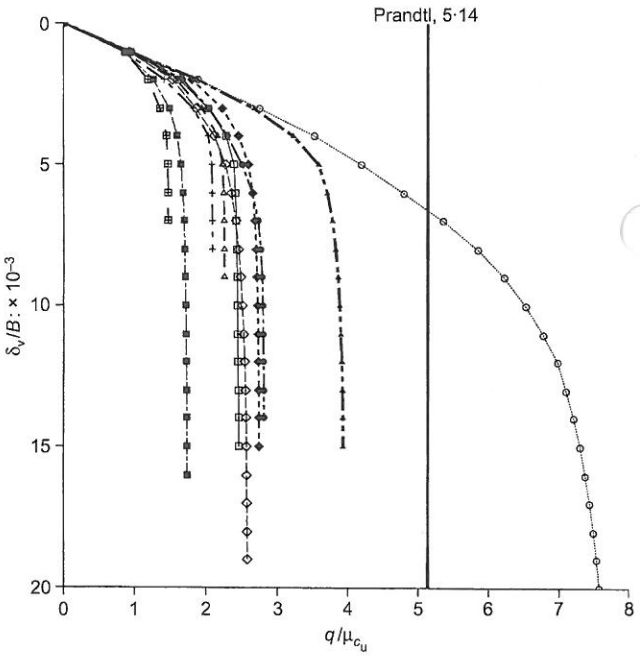

Fig. 3. Typical load/deformation curves corresponding to different realisations in the bearing capacity analysis of an undrained clay with $\Theta_{c_u} = 1$ and $\mathrm{COV}_{c_u} = 1$

for low values of COV_{c_u}, m_{N_c} tends to the deterministic Prandtl value of 5·14. For higher values of COV_{c_u}, however, the mean bearing capacity factor falls steeply, especially for lower values of Θ_{c_u}. For example, in a highly variable case where $\Theta_{c_u} = 0{\cdot}5$ and $\mathrm{COV}_{c_u} = 4$, the predicted m_{N_c} value is less than unity—over five times smaller than the Prandtl value! For the recommended upper limit of $\mathrm{COV}_{c_u} = 0{\cdot}5$ suggested by Lee *et al.* (1983) and others, the m_{N_c} value is closer to 4, corresponding to a more modest reduction of 20%. What this implies from a design standpoint is that the bearing capacity of a heterogeneous soil will on average be less than the Prandtl solution that would be predicted assuming the soil is homogeneous with its strength given by the mean value. The influence of Θ_{c_u} is also pronounced with the greatest reduction from the Prandtl solution being observed with values around $\Theta_{c_u} \approx 0{\cdot}5$. As the value of Θ_{c_u} is reduced further towards zero, there is evidence of a gradual increase in the value of m_{N_c}, as shown in Fig. 6(b). From a theoretical point of view, it could be speculated that, as

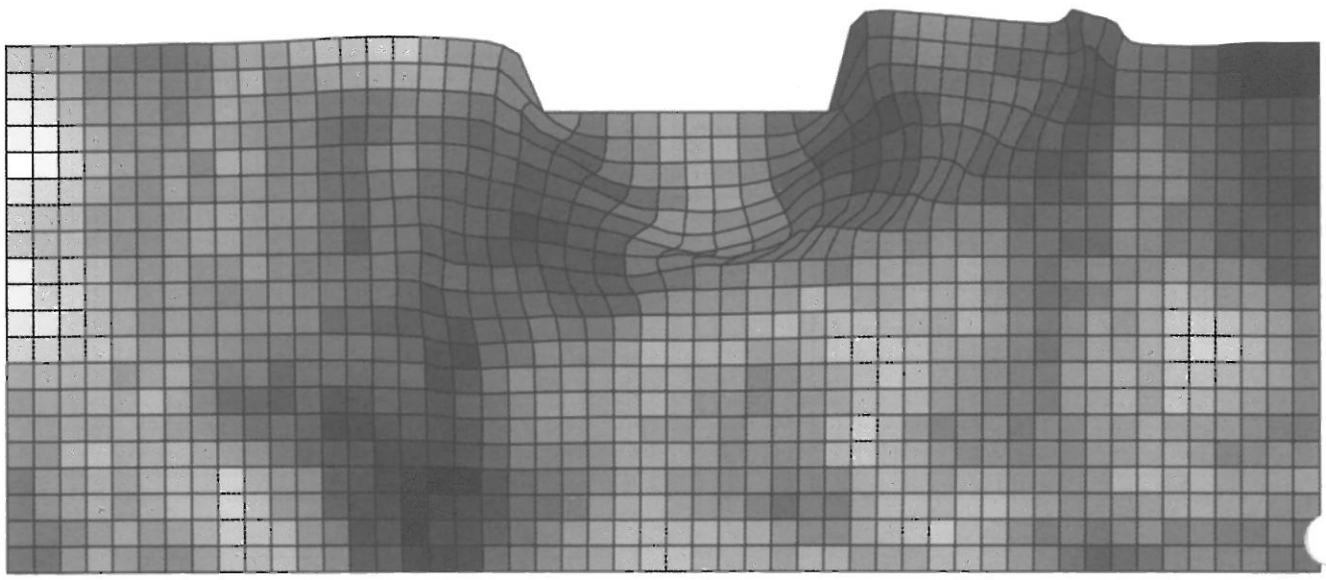

Fig. 4. Typical deformed mesh and greyscale at failure with $\Theta_{c_u} = 1$. The darker regions indicate weaker soil

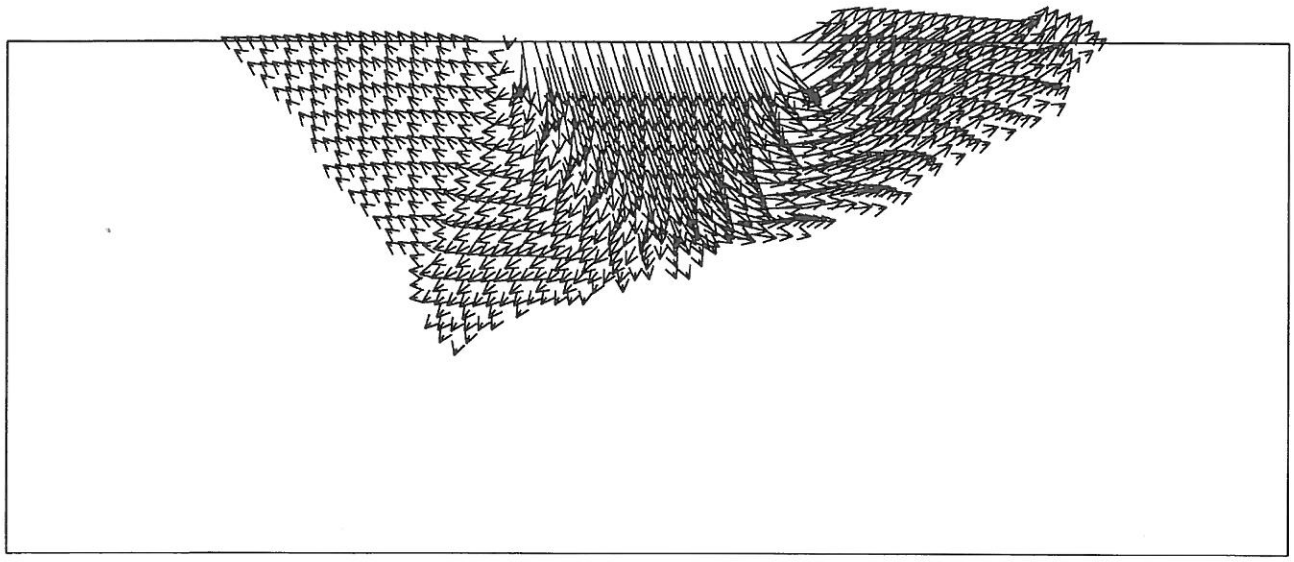

Fig. 5. Displacement vectors at failure for the same case shown in Fig. 4. The non-symmetric shape of the failure mechanism is clearly visible

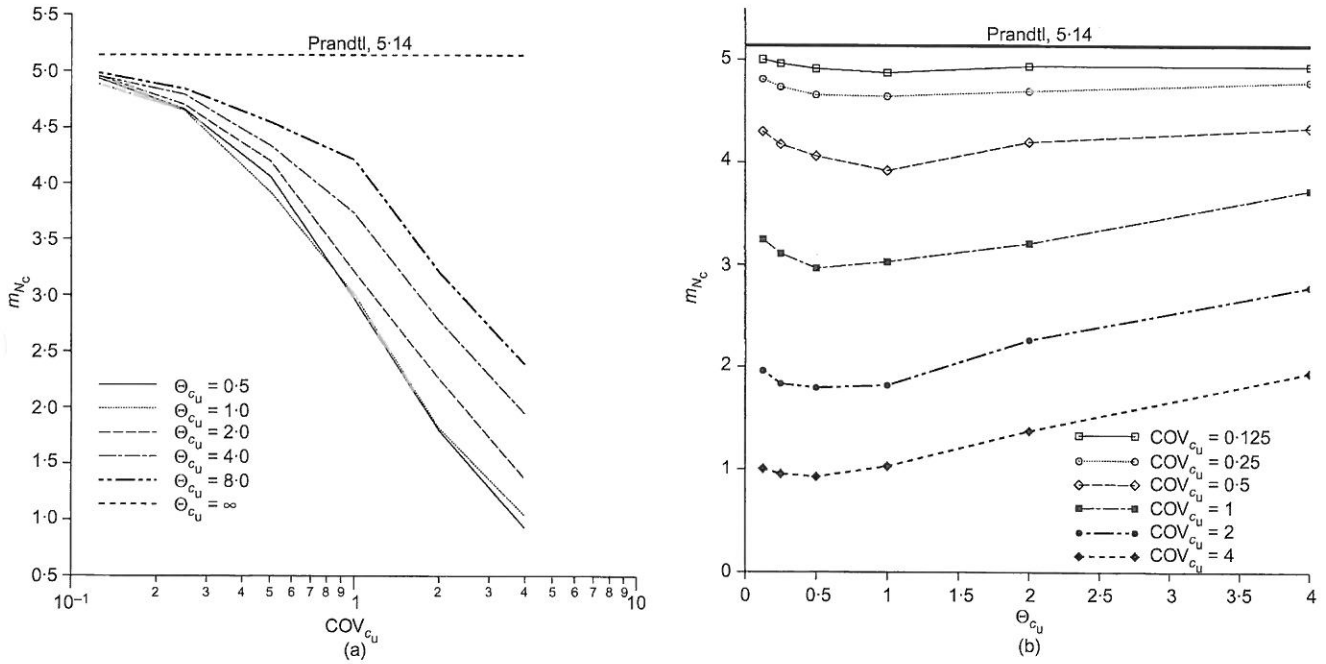

Fig. 6. (a) Estimated mean bearing capacity factor, m_{N_c}, as a function of undrained shear strength statistics, Θ_{c_u} and COV_{N_c}. (b) More clearly shows the increase in m_{N_c} as $\Theta_{c_u} \to 0$

Θ_{c_u} becomes vanishingly small, the mean bearing capacity factor will continue to increase towards the deterministic Prandtl solution of 5·14. The explanation lies in the fact that as the spatial correlation length decreases, the weakest path becomes increasingly tortuous and its length correspondingly longer. As a result, the weakest path starts to look for shorter routes cutting through higher-strength material. In the limit, as $\Theta_{c_u} \to 0$, it is expected that the optimum failure path will be the same as in a uniform material with strength equal to the mean value, hence returning to the deterministic Prandtl solution.

Also included in Fig. 6(a) is a horizontal line corresponding to the analytical solution that would be obtained for $\Theta_{c_u} = \infty$. This hypothetical case implies that each realisation of the Monte Carlo process involves an essentially homogeneous soil, albeit with strength varying only from one realisation to the next. In this case, the distribution of q_f will be statistically similar to the underlying distribution of c_u but magnified by 5·14. The mean bearing capacity will therefore be given by

$$\mu_{q_f} = 5{\cdot}14\mu_{c_u} \tag{15}$$

hence $m_{N_c} = 5{\cdot}14$ for all COV_{c_u}.

Figure 7 shows the influence of Θ_{c_u} and COV_{c_u} on the estimated coefficient of variation of the bearing capacity factor, $COV_{N_c} = s_{N_c}/m_{N_c}$. The plots indicate that COV_{N_c} is positively correlated with both COV_{c_u} and Θ_{c_u}. This figure also indicates that the correlation length, Θ_{c_u}, has a significant influence on COV_{N_c}. For small correlation lengths COV_{N_c} is small and rather insensitive to COV_{c_u}; however, for higher correlation lengths COV_{N_c} increases quite consistently until it reaches the limiting maximum value corresponding to $\Theta_{c_u} = \infty$, defined by the straight line where $COV_{N_c} = COV_{c_u}$.

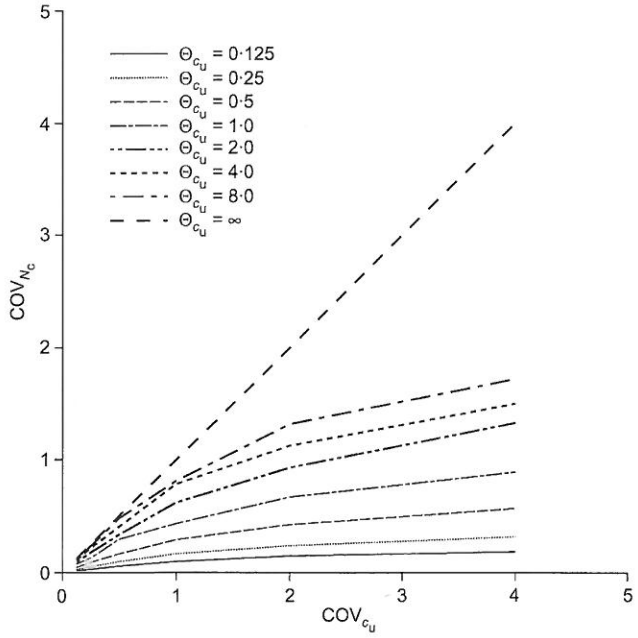

Fig. 7. Estimated coefficient of variation of the bearing capacity factor $COV_{N_c} = s_{N_c}/m_{N_c}$ as a function of undrained shear strength statistics, Θ_{c_u} and COV_{c_u}

PROBABILISTIC INTERPRETATION

Following Monte Carlo simulation for each parametric combination of input parameters (Θ_{c_u} and COV_{c_u}), the suite of computed bearing capacity factor values from equation (4) was plotted in the form of a histogram, and a 'best-fit' log-normal distribution superimposed. An example of such a plot is shown in Fig. 8 for the case where $\Theta_{c_u} = 2$ and $COV_{c_u} = 1$.

Since the log-normal fit has been normalised to enclose an area of unity, areas under the curve can be directly related to probabilities. From a practical viewpoint it would be of interest to estimate the probability of 'design failure', defined here as occurring when the computed bearing capacity is less than the Prandtl value based on the mean strength. That is:

'Design failure' if $q_f < 5{\cdot}14\mu_{c_u}$ (16)

Let this probability be $p(N_c < 5{\cdot}14)$: hence from the properties of the underlying normal distribution we get

$$p(N_c < 5{\cdot}14) = \Phi\left(\frac{\ln 5{\cdot}14 - m_{\ln N_c}}{s_{\ln N_c}}\right) \quad (17)$$

where Φ is the cumulative normal function.

For the particular case shown in Fig. 8, the fitted log-normal distribution has the properties $m_{N_c} = 3{\cdot}31$ and $s_{N_c} = 2{\cdot}08$: hence from equations (5) and (6) the underlying normal distribution is defined by $m_{\ln N_c} = 1{\cdot}03$ and $s_{\ln N_c} = 0{\cdot}58$. Equation (17) therefore gives $p(N_c < 5{\cdot}14) = 0{\cdot}85$, indicating an 85% probability that the actual bearing capacity will be less than the Prandtl value.

Figure 9 gives a summary of $p(N_c < 5{\cdot}14)$ for a range of values of Θ_{c_u} and COV_{c_u}. The figure indicates a wide spread of probability values with respect to Θ_{c_u}, with the highest probabilities corresponding to the lowest values of Θ_{c_u}. For example, a soil with $COV_{c_u} = 0{\cdot}5$ exhibits a range of $0{\cdot}59 < p(N_c < 5{\cdot}14) < 0{\cdot}95$, with the low and high values corresponding to $\Theta_{c_u} = \infty$ and $\Theta_{c_u} = 0{\cdot}5$ respectively.

The influence of COV_{c_u} on the probability is also significant. Theoretically, as $COV_{c_u} \to 0$, the probability $p(N_c < 5{\cdot}14) \to 0{\cdot}5$, irrespective of the value of Θ_{c_u}. The results in Fig. 9 indicate that this convergence occurs faster for higher values of Θ_{c_u} than for lower values. It would appear that low values of Θ_{c_u} permit such widely scattered weak elements that the probability of the actual bearing capacity lying below the Prandtl value remains high, even for low COV_{c_u} values. This general trend is to be expected, however, because for low COV_{c_u} values the distribution of bearing capacity factors becomes 'bunched up' and 'centred' on 5·14, giving an almost equal chance of the computed bearing capacity factor lying on either side of the Prandtl solution.

As COV_{c_u} is increased, the probability $p(N_c < 5{\cdot}14)$ also increases. For example, when $\Theta_{c_u} = 0{\cdot}5$ and $COV_{c_u} = 0{\cdot}5$, $p(N_c < 5{\cdot}14) = 0{\cdot}95$, indicating a 95% probabilty that the actual bearing capacity will be lower than the Prandtl solution.

The result corresponding to the limiting cases of $\Theta_{c_u} = \infty$ is also indicated in Fig. 9. As dicussed previously, the distribution of q_f in this case is statistically similar to the underlying distribution of c_u, and the required probability, $p(N_c < 5{\cdot}14)$, simply equals the area under the probability density function to the left of the mean. For a log-normal distribution this probability is always greater than 0·5, and is given by

$$p(N_c < 5{\cdot}14) = \Phi(0{\cdot}5\sigma_{\ln c_u}) \quad (18)$$

Thus from equation (5):

$$p(N_c < 5{\cdot}14) = \Phi(0{\cdot}5\sqrt{[\ln(1 + COV_{c_u}^2)]} \quad (19)$$

Figure 9 indicates that the expected bearing capacity of a strip footing on an undrained clay with variable shear strength defined by a log-normal distribution will always be lower than the Prandtl value based on the mean strength. It could be argued, however, that this interpretation gives an over-pessimistic impression of the role of soil strength variability by not taking account of the variance of the bearing capacity. Even an essentially deterministic analysis with a very small shear

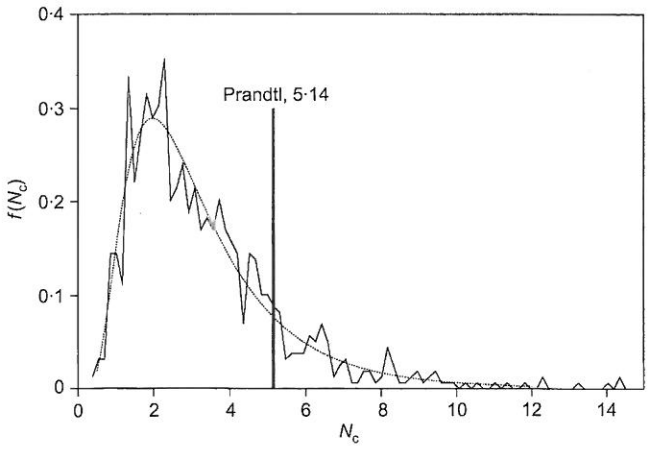

Fig. 8. Histogram and log-normal fit for the computed bearing capacity factors when $\Theta_{c_u} = 2$ and $COV_{c_u} = 1$. The log-normal function has the properties $m_{N_c} = 3{\cdot}31$ and $s_{N_c} = 2{\cdot}08$

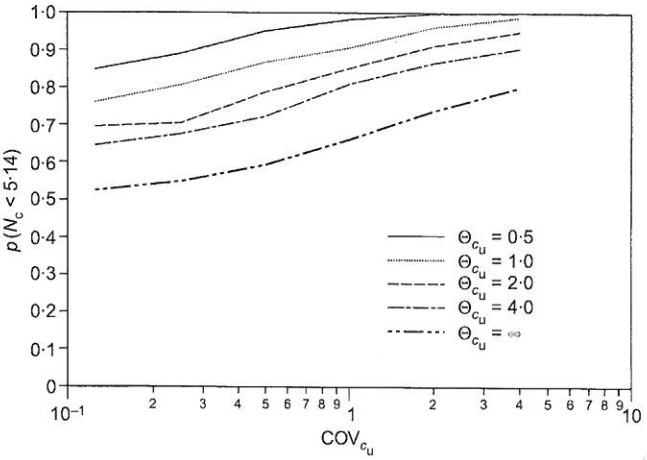

Fig. 9. Graph showing the probability $p(N_c < 5{\cdot}14)$ that the bearing capacity factor will be lower than the Prandtl solution based on the mean strength

strength variance would suggest a 50% probability that the bearing capacity would lie below the Prandtl value.

In order to remove this anomaly, the results have been reinterpreted in Figs 10 and 11 to compare the computed bearing capacity factor with the Prandtl solution after it has been reduced by a factor F. The factor F is equivalent to a factor of safety applied to the deterministic bearing capacity based on mean strength. The probability of design failure in the form of $p(N_c < 5{\cdot}14/F)$ is now greatly reduced, giving a more reassuring result from a design viewpoint. For example, from Fig. 10 in which $F = 2$, the probability of design failure for a soil with $\Theta_{c_u} = 1$ and $\mathrm{COV}_{c_u} = 0{\cdot}5$ is about 6%. This probability is essentially reduced to zero for the same soil by increasing the factor to $F = 3$, as shown in Fig. 11.

Figure 12 shows more clearly how F affects the probability of design failure for a range of COV_{c_u} in a soil where the correlation length is held constant at $\Theta_{c_u} = 1$. The results indicate that quite high factors of safety are required to reduce the probability of design failure to acceptable levels. Fig. 12 also shows that for a soil with $\mathrm{COV}_{c_u} = 0{\cdot}5$ and $\Theta_{c_u} = 1$, a factor of safety of at least 3 is needed to essentially eliminate all probability of design failure. This is consistent with geotechnical engineering practice, where a factor of safety of at least 3 (e.g. Lambe & Whitman, 1969) is considered necessary to protect against general shear failure.

A further interpretation of the probability of design failure is shown in Fig. 13, where a direct comparison is given between the probability of design failure $p(N_c < 5{\cdot}14/F)$ and the factor of safety, F, for a range of Θ_{c_u} and COV_{c_u} values.

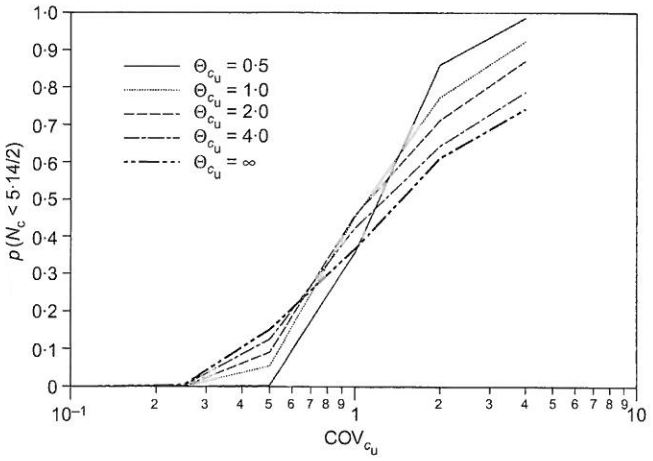

Fig. 10. Graph showing the probability $p(N_c < 5{\cdot}14/2)$ that the bearing capacity factor will be lower than the Prandtl solution based on the mean strength incorporating a factor of safety $F = 2$

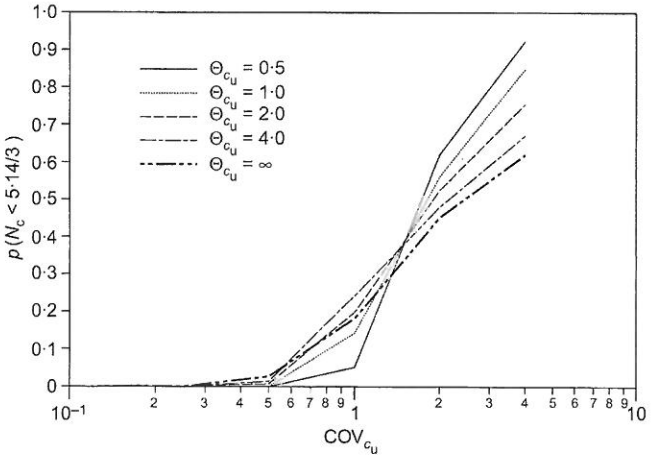

Fig. 11. Graph showing the probability $p(N_c < 5{\cdot}14/3)$ that the bearing capacity factor will be lower than the Prandtl solution based on the mean strength incorporating a factor of safety $F = 3$

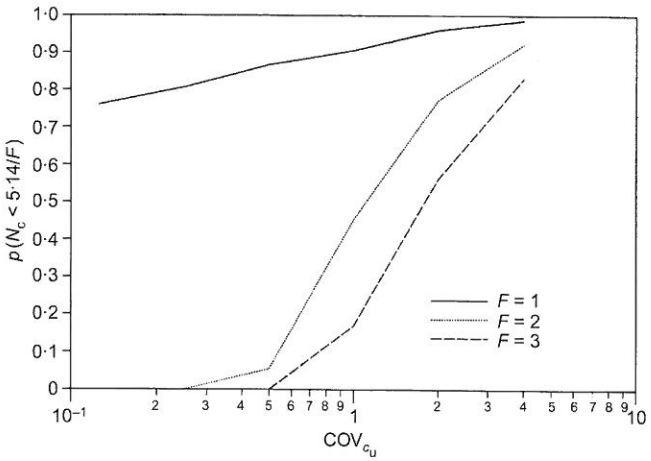

Fig. 12. Graph showing the probability $p(N_c < 5{\cdot}14/F)$ that the bearing capacity factor will be lower than the Prandtl solution based on the mean strength for three different factors of safety, F, for a soil with $\Theta_{c_u} = 1$

If the goal is to virtually eliminate any possibility of design failure involving a bearing capacity calculation based on the mean strength, Fig. 13(a) indicates that for a soil with $\mathrm{COV}_{c_u} = 0{\cdot}125$ (a value at the lower end of the recommended range of Lee *et al.*, 1983, and others), a factor of safety of $F = 1{\cdot}5$ would be needed. For an intermediate value of $\mathrm{COV}_{c_u} = 0{\cdot}25$, the required factor of safety becomes $F = 2$ (Fig. 13(b)), and for a soil with $\mathrm{COV}_{c_u} = 0{\cdot}5$ (a value at the upper end of the recommended range), the required factor of safety increases further to $F = 3$, as shown in Fig. 13(c). In the case of $\mathrm{COV}_{c_u} = 1$ (Fig. 13(d))—a value that might be considered exceptionally high for most soils—the need for even higher factors of safety is indicated.

An important observation from Fig. 13 is that the correlation length, Θ_{c_u}, becomes increasingly relevant to the probabilistic interpretation of the bearing capacity problem as COV_{c_u} gets larger. This is clear from the way the curves are bunched together when $\mathrm{COV}_{c_u} = 0{\cdot}125$ (Fig. 13(a)) yet are quite divergent when $\mathrm{COV}_{c_u} = 1$ (Fig. 13(d)).

In all of Fig. 13, the 'crossing-over' of the lines corresponding to different Θ_{c_u} values implies that high values of Θ_{c_u} are beneficial to design at low values of F by giving lower probabilities of design failure, but may be a liability at higher values of F. The explanation lies in the fact that smaller correlation lengths lead to smaller values of COV_{N_c}, as shown in Fig. 7. Increasing F will therefore result in a steeper fall in the probability of design failure as the factored bearing capacity factor rapidly passes through the 'bunched up' distribution.

In addition to the expected trend, which shows $p(N_c < 5{\cdot}14/F)$ decreasing as F increases for all Θ_{c_u}, the curves also confirm that a factor of safety of 3 is able to reduce the probability of design failure to negligible levels for all soils in the recommended range of $0{\cdot}1 < \mathrm{COV}_{c_u} < 0{\cdot}5$. These results may help explain, in a probabilistic context, why factors of safety used in bearing capacity calculations are typically much higher than those used in other limit state calculations in geotechnical engineering, such as slope stability and earth pressures.

CONCLUDING REMARKS

The paper has shown that soil strength heterogeneity in the form of a spatially varying log-normal distribution can significantly reduce the mean bearing capacity of a strip footing on undrained clay.

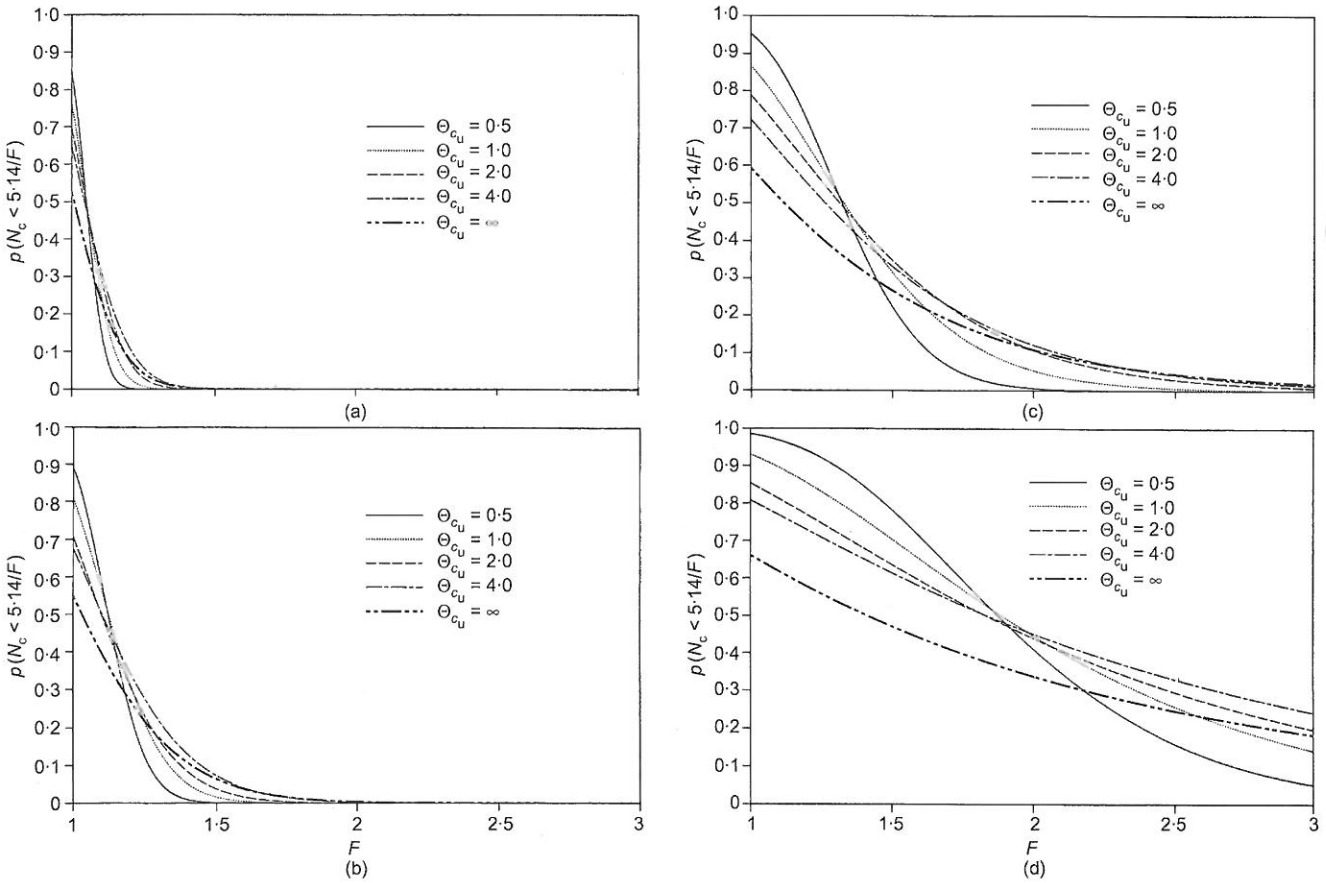

Fig. 13. Graphs showing the relationship between $p(N_c < 5{\cdot}14/F)$ and F for a soil with COV_{c_u} = (a) 0·125, (b) 0·25, (c) 0·5 and (d) 1

The following more specific conclusions can be made:

(*a*) As the variance of soil strength increases, the mean bearing capacity decreases. A minimum mean bearing capacity was observed for correlation lengths of approximately one half of the footing width. For still smaller correlation lengths, a modest increase in the mean bearing capacity was detected. It could be speculated that, as Θ_{c_u} becomes vanishingly small, the mean bearing capacity factor will continue to increase towards the deterministic Prandtl solution of 5·14. The explanation may lie in the fact that, with no spatial correlation, there are no preferred paths of weaker material to attract the mechanism, and the material response is 'homogeneous', yielding an essentially deterministic symmetric mechanism at failure.

(*b*) The coefficient of variation of the bearing capacity was observed to be positively correlated with both the coefficient of variation of the soil strength and its spatial correlation length.

(*c*) Results have been presented in a probabilistic context to determine the probability of design failure, defined as the probability that the actual bearing capacity would be lower than a factored deterministic prediction of bearing capacity using Prandtl's formula based on the mean strength of the soil.

(*d*) By investigating the role of a factor of safety applied to the Prandtl solution, it was observed that a value of $F = 3$ would essentially eliminate any possibility of design failure for soils with a strength variability within the recommended range.

(*e*) The influence of correlation length on the probabilistic interpretations of the bearing capacity problem was shown to be significant, especially for soils with higher values of COV_{c_u}.

ACKNOWLEDGEMENTS

The writers acknowledge the support of NSF Grant No. CMS-9877189 and the support of the Natural Sciences and Engineering Research Council of Canada Operating Grant No. OGP0105445.

NOTATION

B	footing width
COV_{c_u}	coefficient of variation of undrained shear strength
COV_{N_c}	estimated coefficient of variation of bearing capacity factor
c_u	undrained shear strength
c_{u_i}	undrained shear strength assigned to ith element
E	Young's modulus
F	factor of safety
$f(..)$	probability density function
g	standard Gaussian field (zero mean, unit variance)
g_i	local average of Gaussian field over ith element
i, j	integers that count realisations or elements
m_{N_c}	estimated mean of bearing capacity factor
$m_{\ln N_c}$	estimated mean of log bearing capacity factor
N_c	Prandtl bearing capacity factor
N_{c_i}	Prandtl bearing capacity factor of ith realisation
n_{sim}	number of Monte Carlo realisations
$p(..)$	probability
Q_i	footing reaction force of ith realisation
Q_{f_i}	footing reaction force at bearing failure of ith realisation
q	average footing stress
q_f	footing bearing capacity
q_{f_i}	footing bearing capacity of ith realisation
s_{N_c}	estimated standard deviation of bearing capacity factor
$s_{\ln N_c}$	estimated standard deviation of log bearing capacity factor
δ_v	vertical displacement of rigid footing
Θ_{c_u}	dimensionless spatial correlation of log undrained shear strength
θ_{c_u}	spatial correlation of undrained shear strength

$\theta_{\ln c_u}$ spatial correlation length of log undrained shear strength
μ_{c_u} mean of undrained shear strength
$\mu_{\ln c_u}$ mean of log undrained shear strength
μ_{q_f} mean bearing capacity
ν Poisson's ratio
ρ correlation coefficient
σ_{c_u} standard deviation of undrained shear strength
$\sigma_{\ln c_u}$ standard deviation of log undrained shear strength
τ distance between two points in random field
$\Phi(..)$ cumulative normal function
ϕ_u undrained friction angle

REFERENCES

Asaoka, A. & Grivas, D. A. (1982). Spatial variability of the undrained strength of clays. *J. Geotech. Engng, ASCE* **108**, No. 5, 743–756.

de Marsily, G. (1985). Spatial variability of properties in porous media: a stochastic approach. In *Advances in transport phenomena in porous media* (eds J. Bear and M. Y. Corapcioglu), pp. 719–769. Boston: Dordrecht. NATO Advanced Study Institute on Fundamentals of Transport Phenomena in Porous Media.

DeGroot, D. J. & Baecher, G. B. (1993). Estimating autocovariance of in-situ soil properties. *J. Geotech. Engng, ASCE* **119**, No. 1, 147–166.

Duncan, J. M. (2000). Factors of safety and reliability in geotechnical engineering. *J. Geotech. Geoenviron. Engng, ASCE* **126**, No. 4, 307–316.

Fenton, G. A. (1990). *Simulation and analysis of random fields*. PhD thesis, Department of Civil Engineering and Operations Research, Princeton University.

Fenton, G. A. (1999). Random field modeling of CPT data. *J. Geotech. Geoenviron. Engng, ASCE* **125**, No. 6, 486–498.

Fenton, G. A. & Vanmarcke, E. H. (1990). Simulation of random fields via local average subdivision. *J. Engng Mech., ASCE* **116**, No. 8, 1733–1749.

Griffiths, D. V. & Fenton, G. A. (1997). Three-dimensional seepage through a spatially random soil. *J. Geotech. Engng, ASCE* **123**, No 2, 153–160.

Harr, M. E. (1987). *Reliability based design in civil engineering*. New York: McGraw-Hill.

Hoeksema, R. J. & Kitanidis, P. K. (1985). Analysis of the spatial structure of properties of selected aquifers. *Water Resour. Res.* **21**, No. 4, 563–572.

Kulhawy, F. H., Roth, M. J. S. & Grigoriu, M. D. (1991). Some statistical evaluations of geotechnical properties. *Proc. 6th Int. Conf. Appl. Stats. Prob. Civ. Eng.* Mexico City, **2**, pp. 705–712.

Lambe, T. W. & Whitman, R. V. (1969). *Soil mechanics*. Chichester/New York: John Wiley & Sons.

Lee, I. K., White, W. & Ingles, O. G. (1983). *Geotechnical engineering*. London: Pitman.

Smith, I. M. & Griffiths, D. V. (1998). *Programming the finite element method*, 3rd edn. Chichester/New York: John Wiley & Sons.

Sudicky, E. A. (1986). A natural gradient experiment on solute transport in a sand aquifer: spatial variability of hydraulic conductivity and its role in the dispersion process. *Water Resour. Res.* **23**, No. 13, 2069–2083.

Vanmarcke, E. H. (1984). *Random fields: analysis and synthesis*. Cambridge, MA: MIT Press.